Puneet Kumar Gupta ✉
N.P. Yadav

https://doi.org/10.21278/TOF.482056023
ISSN 1333-1124
eISSN 1849-1391

NUMERICAL INVESTIGATION INTO CONVECTIVE HEAT TRANSFER COEFFICIENT OF THE GRINDING FLUID USED IN A DEEP GRINDING PROCESS

Summary

This paper presents a mathematical modelling approach to an investigation into the grinding temperature and the convective heat transfer coefficient of the grinding fluid using the computational fluid dynamics approach. The maximum grinding temperature varies from 325 K to 370 K as the grinding depth increases from 0.50 mm to 1.10 mm at 60 m/s wheel velocity for water as a grinding fluid and 419 K to 619 K for kerosene oil as a grinding fluid. The convective heat transfer coefficient depends on the density, specific heat, conductivity, and viscosity of the grinding fluid. It is observed that the value of the convective heat transfer coefficient increases with an increase in density, specific heat, and conductivity of the grinding fluid and decreases with an increase in viscosity of the grinding fluid. The convective heat transfer coefficient for water and kerosene oil is 137,730 W/m^2-K and 23,512 W/m^2-K, respectively, at a 76 m/s wheel velocity and 0.50 mm depth of cut.

Key words: *computational fluid dynamics (CFD); grinding temperature; convective heat transfer coefficient; grinding fluid properties*

1. Introduction

Researchers are continuously working on improvements to manufacturing processes to achieve high dimensional accuracy and a high degree of surface smoothness. Grinding is one of the manufacturing processes in which an abrasive wheel is used to remove fine quantities of material with high dimensional accuracy so as to achieve a high degree of smoothness of the workpiece surfaces. In the creep-feed process, the workpiece speed is lower and the grinding depth is higher in a single pass of the grinding wheel. So, the workpiece speed can be as low as 0.001 m/s, while the grinding depth can be even more than 0.5 mm. However, in conventional grinding, the work speed is of the order of 0.1 m/s, and the grinding depth is 10 micrometers [1]. In this process, the energy is directly converted into heat, material deformation, and chip acceleration; consequently, much heat is generated. Hence, the temperature significantly increases in the grinding zone, reducing the workpiece surface quality. The high heat generation in the grinding zone leads to sparks, tempering, burning, and heat checking on the surfaces, and residual stresses are generated. Therefore, the challenges for the researcher are to get a high degree of surface smoothness and dimensional accuracy by analysing the thermal aspects during the grinding process. Using a grinding fluid is one of the best ways to control the grinding temperature. Sufficient cooling is necessary in the case of a deep or creep-feed grinding process. The fluids are used in the machining process for two purposes: cooling and lubricating. These fluids can be categorized as water-based coolants and oil-based coolants. The selection of a grinding fluid for a particular grinding process is an important aspect. So, the present study focused on the study of the performance of water-based and oil-based grinding fluids in the deep grinding process. The grinding fluids are vital in the convection heat transfer as they reduce the grinding temperature. There are various factors on which the convective heat transfer coefficient of the grinding fluid depends.

Jin and Stephenson [2] explained that the coefficient of the convective heat transfer of grinding fluids is dependent on wheel velocity and increases with wheel velocity. Zhang et al. [3] explained how convection heat transfer through the grinding fluid can be improved. The convection heat transfer of the grinding fluid is predominant at higher wheel velocities. Jin and Stephenson [4] presented a model of transient heat transfer for high-efficiency deep grinding conditions. It was observed that heat transfer for steady-state conditions is achieved for high-efficiency deep grinding conditions after achieving a maximum contact length. Zhang et al. [5] discussed the convection heat transfer through grinding fluids based on the heat transfer theory. They suggested that by increasing the wheel velocity and decreasing the workpiece speed, the lubrication effect of the grinding fluid can be obtained.

Peng et al. [6] explained convective cooling in high-speed grinding and suggested that a high convective heat transfer coefficient of the grinding fluid is identified at high wheel speeds. Rowe et al. [7] developed thermal modelling using various critical factors to control thermal damage. It was observed that grinding at high speeds is more beneficial to avoid the bulk temperature rise because there is a huge reduction in the cycle for high-speed grinding. Liao and Yanga [8] reported that the grinding fluid flow rate is sufficient to reduce the grinding zone thermal boundary layer under general grinding conditions. Contact time is large in the case of creep-feed grinding between grinding fluid and workpiece, resulting in the dissipation of a large amount of heat. Marios and Lavine [9] reported the dependency of the maximum temperature on some unknown geometric parameters, such as a fraction of active grains, the grain sharpness, and the shear plane angle. The maximum temperature decreases as these values increase. O'Donovan et al. [10] suggested the impingement of the jet to enhance heat transfer through convection. It was noticed that providing sufficient cooling penetration of the high-speed jet around the wheel is effective. The distance of a high-speed jet from the grinding zone should be less for better cooling. Tu et al. [11] investigated the grinding process for cast iron and observed that the cutting force and residual stresses depend on the wheel speed and depth of cut. The cutting force and residual stresses are directly proportional to the depth of the cut, whereas they are inversely proportional to speed. Upadhyaya and Malkin [12] discussed the energy partition of 3 to 5% for hardened bearing steel, and a 120 grit electroplated cubic boron nitride (CBN) wheel ground below the burnout temperature. It was observed that the wheel surface shallow porosity could provide sufficient cooling of the grinding zone of the workpiece. Schieber et al. [13] presented a model to predict the thermal aspect of profile grinding. The mechanical load increases directly in the grinding zone in the case of a higher grinding depth because of a large interaction between the workpiece and abrasive grains. Lin et al. [14] studied the coefficient of convective heat transfer for the grinding fluid and suggested that this value decreases as the grinding depth increases. Gupta and Yadav [16] discussed the results of a study including various parameters that affect the value of temperature in the grinding zone for different types of steels using the CFD approach and concluded that the maximum grinding temperature is directly proportional to the grinding depth. Mihic et al. [17] analysed the grinding model for different parameters of coolants. They discussed how the maximum grinding temperature varies with different coolant properties, such as specific heat, density, conductivity, etc. They explained the variation of wheel velocity at maximum grinding temperature; as the wheel velocity increases, the maximum grinding temperature decreases. Jamshidi and Budak [18] developed a thermal model for the grinding process by considering a periodic heat source for dry and wet grinding. They explained that the grinding force has an oscillating nature and hence the produced fluctuation causes a discontinuous heat source. This fluctuation heat source causes an increase in the maximum grinding temperature as compared to the case of a constant heat source. Gupta and Yadav [19] discussed how grinding temperature affects structural properties of the workpiece in the deep grinding process. They found that residual stresses and thermal strain depend on the grinding temperature of the workpiece. As the grinding temperature increases, these values also increase. Xiao et al. [20] explained that sintered porous aggregated CBN wheels exhibit lower grinding temperatures and a lower grinding force as compared to vitrified monocrystalline CBN wheels. Jamshidi and Budak [24] developed a model to predict the surface burn and its width, considering temperature and time exposure. They found that metal burn correlated directly with metal oxidation, and they defined the surface burn in terms of the chemical reaction between oxygen and workpiece material. Ma et al. [25] combined the grinding force and the temperature model of thermal prediction in the face gear grinding. The force model was developed using a single-grain model when grinding fluid was used. The temperature model was developed by considering heat flux and cross-section area of undeformed chip thickness. Thanedar et al. [26] developed an analytical model of temperature to predict the grinding burn. They also observed that minimum thermal damage occurs at higher wheel speeds and lower grinding depths. Zhang and Rowe [27] compared the thermal model of turbulent flow with the laminar thermal model. They suggested that temperature can be reasonably predicted by the turbulent flow thermal model within the fluid boiling temperature limit. Barjesic et al. [31] explained the instability of the grinding process due to the grinding wheel regeneration. Still, there may be some stable regions even at high wheel speeds, and they discussed various parameters to avoid chatter vibration. Todic et al. [32] increased the vanadium content and concluded that hardness decreases slightly, whereas impact toughness increases significantly. Li et al. [33] proposed a belt heating model for conduction heating and calculated the formation temperature during preheating. Chen et al. [34] explained the factors that affect the strength of the cutting edge. These factors are tensile strength, yield strength, shear strength, hardness, and thermal conductivity of the workpiece material.

The literature review shows that in the case of the grinding process, the main concern is how to control the grinding temperature. For the deep grinding process, it becomes most important to control the grinding temperature. Sufficient cooling by a grinding fluid is necessary in the case of a deep grinding process to avoid burnout situations. Cooling can be enhanced by convection heat transfer through the grinding fluid. This study aims to explore how convection heat transfer can be enhanced in the deep grinding process. Enhancing convection heat transfer through a grinding fluid can restrict the high value of the grinding temperature and thus the burnout situation. So, the present study focuses on developing a new method for finding the convective heat transfer coefficient of the grinding fluid and improving the convective heat transfer coefficient of the grinding fluid. Also, the study focuses on providing information related to the selection of the fluid with respect to the thermo-physical properties of the grinding fluid, maximum grinding temperature, and convective heat transfer coefficient of the grinding fluid. This study is based on the computational fluid dynamics approach, which is one of the novel ways of finding the convective heat transfer coefficient. This approach allows the visualisation of the temperature variation on the surface of the workpiece as well as the estimation of the maximum temperature for different varying properties of the grinding fluid, which is not easy to achieve experimentally. This analysis also reduces the number of experiments, costs, and time. Further performance of different types of grinding fluids used in the deep grinding process is also evaluated.

So, this paper focuses on the computational fluid dynamics simulation to investigate the convective heat transfer coefficient of grinding fluids. Various factors are analysed to enhance the convection heat transfer in the deep grinding process. The mathematical modelling of heat transfer in the grinding process is performed in the presence of a cooling fluid. The heat transfer phenomenon is analysed by temperature variation in the grinding zone at different grinding wheel velocities with variable depths of cuts. The maximum temperature and the convective heat transfer coefficient are calculated to understand the cooling behavior during grinding.

2. Mathematical modelling

2.1 Momentum equation

The movement of the grinding fluid in the grinding process depends on wheel velocity and abrasive grain present on the periphery of the wheel. Moving the wheel changes the kinetic energy when the grinding fluid strikes the wheel, and abrasive grains offer restriction in the movement of the grinding fluid. For steady and incompressible flow, the equation used to estimate the flow behaviour can be written as in Eq. (1) [15, 23].

$$S_i = -\left(\frac{\mu}{\alpha}\cdot v_i + C_2\cdot\rho\cdot|v|\cdot v_i\right) \tag{1}$$

where S_i is defined as the source term for the *i*-th (x, y or z) momentum equation, $|v|$, α, μ and C_2 represent the velocity, permeability, fluid viscosity, and inertial resistance factor, respectively.

2.2 Energy equation

The equation for the energy in the contact zone is written as discussed in the literature as in Eq. (2) [15, 23].

$$\nabla\cdot\left(\vec{v}\left(\rho_f E_f + \rho\right)\right) = \nabla\cdot\left[k_{eff}\nabla T - \left(\sum_i h_i J_i\right) + \left(\bar{\bar{\tau}}\cdot\vec{v}\right)\right] + S_f \tag{2}$$

2.3 Modelling of heat generation

The grinding zone heat generation is caused by the grains rubbing the workpiece. The final equation of the generated heat in the grinding zone depends on the velocity ratio, grinding depth, wheel, workpiece material, and diameter.

The final strength total heat source (q') can be calculated as in Eq. (3) [15].

$$q' = \frac{v_p}{v_t}\cdot a^{(3/2)}\cdot D_t^{(1/2)}\cdot k_{vm} \tag{3}$$

where, v_p is the workpiece velocity, v_t is the wheel velocity, D_t is the diameter of the wheel, '*a*' is the grinding depth, and k_{vm} is defined as the specific main grinding resistance, which can be defined as given in Eq. (4).

$$k_{vm} = \frac{C_k}{\varepsilon_k\sqrt{A}} \tag{4}$$

Parameters C_k and ε_k are given in Table 3 [15].

2.4 Modelling of energy partition

The total generated heat in the grinding zone is transferred to the wheel, workpiece, fluid, and chip as given in Eq. (5) [21].

$$q' = q_W + q_s + q_{fluid} + q_{chip} \tag{5}$$

The portion of heat flux q_{fluid} can be expressed as given in Eq. (6) [21].

$$q_{fluid} = h_{fluid} \cdot T_{\max} \tag{6}$$

The portion of heat flux q_W transferred to the workpiece can be expressed as given in Eq. (7) [21].

$$q_W = \frac{\beta_W}{C} \cdot \sqrt{\frac{v_p}{l_c}} \cdot T_{\max} \tag{7}$$

where, β_w can be expressed as given in Eq. (8).

$$\beta_w = \sqrt{k \rho c} \tag{8}$$

where k, c and ρ represent the conductivity, specific heat and density of the workpiece, respectively. C is the constant that depends upon the Peclet number. Its value is 1 for conventional grinding and less than 1 for the deep grinding process [21]. The contact length l_c depends on the grinding depth and effective diameter of the wheel, and for a deep cut, it can be expressed as given in Eq. (9).

$$l_c = \sqrt{a \cdot D_e} \tag{9}$$

The portion of heat flux q_s transferred in the grinding wheel is given in Eq. (10) [21].

$$q_s = q_W \frac{k_g}{\beta_W \sqrt{r_a v_t}} \tag{10}$$

where k_g is defined as the conductivity of abrasive grains, v_t represents the wheel velocity, and r_o represents the effective radius of contact of abrasive grains. Its value may be taken as 10 microns for a reasonably sharp wheel [21]. For the heat partitioning model, CBN is used as abrasive grain with properties given in Table 4 [21]. The porosity of the wheel is taken as 0.50, as suggested by Mihic et al. [15].

The portion of heat flux transferred to the chip can be calculated by Eq. (11) as suggested by Row et al. [21], where T_{chip} is the material melting temperature.

$$q_{chip} = \left(\frac{\rho \cdot c \cdot a \cdot v_p}{l_c} \right) \cdot T_{chip} \tag{11}$$

The portion of heat transfer through the grinding fluid depends on the type of grinding fluid. Hence, the convective heat transfer coefficient can be expressed as in Eq. (12).

$$h_{fluid} \cdot T_{\max} = q' - (q_W + q_s + q_{chip}) \tag{12}$$

3. Numerical simulation

3.1 Geometrical specification

The flow domain of the process is defined as a rotating grinding wheel, a grinding zone, an upper layer of the workpiece, a shield, and a nozzle (circular cross section) as the inlet of the grinding fluid. In this study, the geometrical specifications are as follows: the workpiece area is 0.580 m x 0.150 m, the wheel diameter is 0.340 m, the area of the grinding zone is 0.05 m x 0.030 m, the shield radius is 0.180 m, the grinding depth is taken as 1 mm, the nozzle diameter is 5 mm and the width of the wheel is taken as 0.050 m. The geometry of the grinding process and the meshed geometry used for the simulation and the positioning of the grinding zone are shown in Fig. 1.

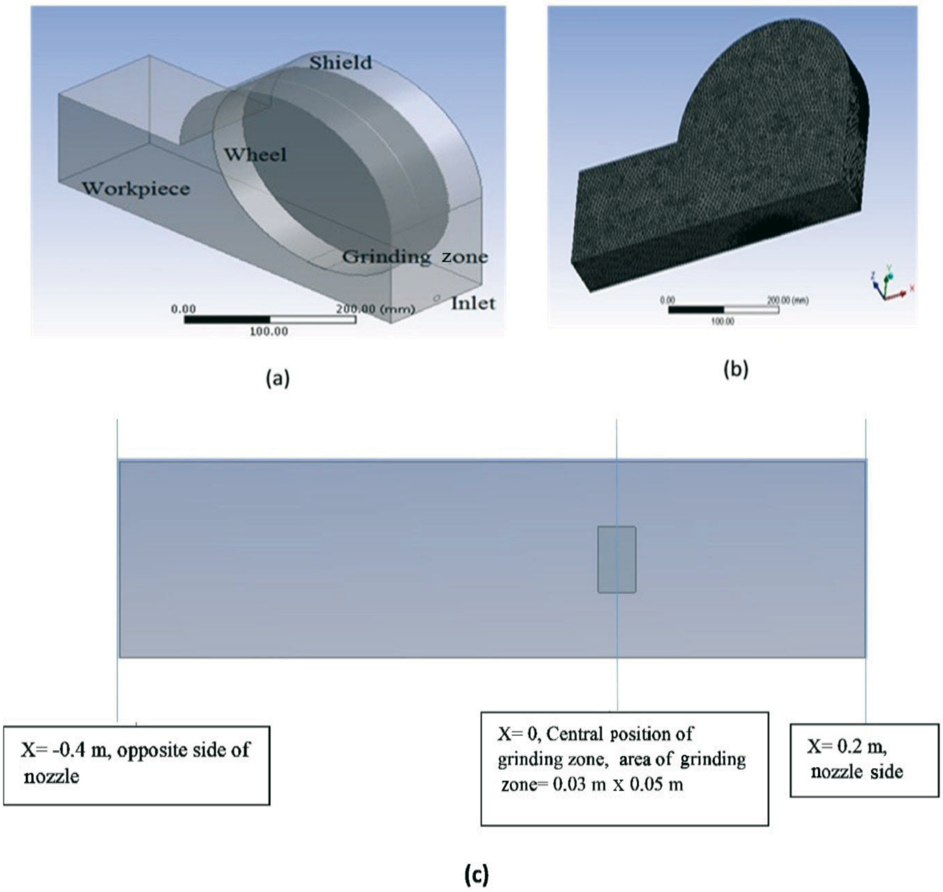

Fig. 1 (a) Grinding process geometry (b) Geometry with meshing (c) Workpiece

3.2 Boundary conditions

The study deals with a CFD approach to the thermal analysis of the grinding process. The grinding process deals with fluid movement, energy generation, and transfer. The grinding fluid comes from the inlet and strikes the grinding zone. The grinding region is a contact region where heat is generated. The rotating grinding wheel rotates in a clockwise direction. The parameters used in this analysis are given in Table 1. The inlet is assigned the inlet velocity of the grinding fluid. In this analysis, water and kerosene oil are used as grinding fluids. A CBN wheel is used as abrasive material. The properties of the grinding fluids and parameters of the CBN wheel are given in Table 2. The grinding zone is assumed to be a porous zone with a porosity of 0.5. The heat input is provided in the grinding zone. The heat input value is estimated from the heat generation model and it depends on various manufacturing parameters, such as wheel velocity, workpiece velocity, grinding depth, diameter of the wheel, and workpiece material. Aluminium is used as a workpiece material. The parameters for finding the specific main grinding resistance for materials are given in Table 3. Initial conditions are taken as atmospheric. The maximum grinding temperature is evaluated applying the CFD approach, and the convective heat transfer coefficient can be estimated by using the energy partition model. A detailed schematic of the grinding process is given in Fig. 2.

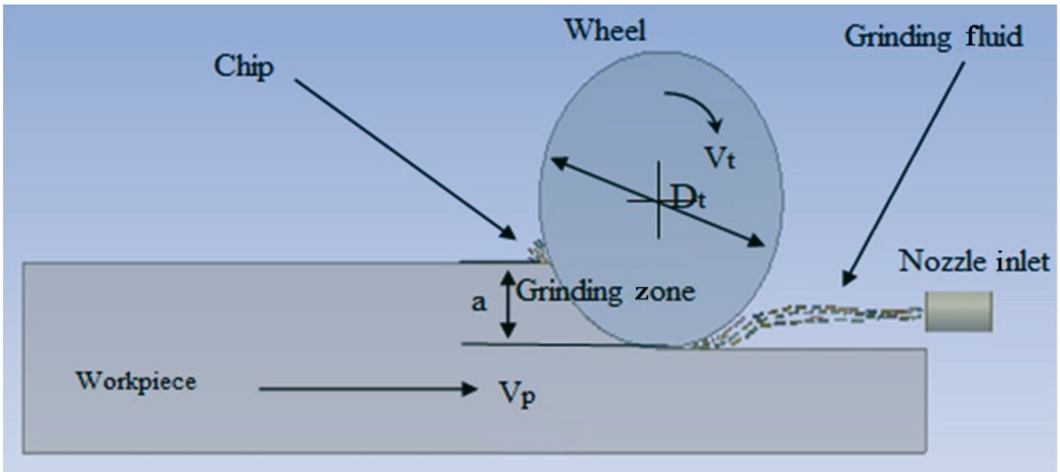

Fig. 2 Schematic and boundaries of grinding process

3.3 Numerical model

The simulation is performed by the Ansys Inc. FLUENT 19.0 R3 software. The major assumptions in the analysis are the pressure-based steady-state flow, the absolute velocity formulation, and the turbulent flow behaviour. The second-order upwind is used for momentum, pressure, Reynolds stress, energy, turbulent kinetic energy, and dissipation rate. The coupled scheme is used. The Reynolds stress model is used for turbulence flow. The convergence criteria are set as 10^{-6} for energy and 10^{-3} for other quantities, as recommended in literature [15, 23].

Table 1 Parameters of the study

Parameters	Simulation specification
Wheel velocity	60, 68, 76 m/sec
Grinding fluid velocity	20 m/sec
Workpiece velocity	1 mm/sec
Grinding depth	0.50, 0.70, 0.90, 1.10 mm
Grinding fluid	kerosene, water
Workpiece	aluminium

Table 2 Properties of grinding fluid [23] and properties of abrasive grains CBN [21]

	Kerosene oil	Water	CBN
Specific heat (J/kgK)	2,090	4,182	506
Density (kg/m^3)	780	998.2	3,480
Viscosity (kg/m-sec)	0.0024	0.00103	-
Conductivity (W/m-K)	0.149	0.6	240

Table 3 Materials parameters C_k and ε_k [15].

	C_k	ε_k
Carbon steel	$1.936 \cdot 10^8$	6.1
Brass	$0.9 \cdot 10^8$	6.8
Aluminium	$1.92 \cdot 10^8$	8

4. Grid independency test and model validation

4.1 The grid independency test

The grid independency test is performed to obtain an optimum number of mesh elements. An unstructured tetrahedron mesh is selected for the present study. The study is performed for five different numbers of elements, as shown in Fig. 3. Parameters for the grid independence test and validation are taken from literature [15] as follows: wheel velocity is 20.4 m/s, inlet velocity of the grinding fluid (water) is 15.5 m/s, grinding depth is 1 mm and energy input (W/mm^2) parameters are taken as 2, 4, 6, and 8. Therefore, the optimum number of elements, 520,473, was used for further study as per the grid independence test.

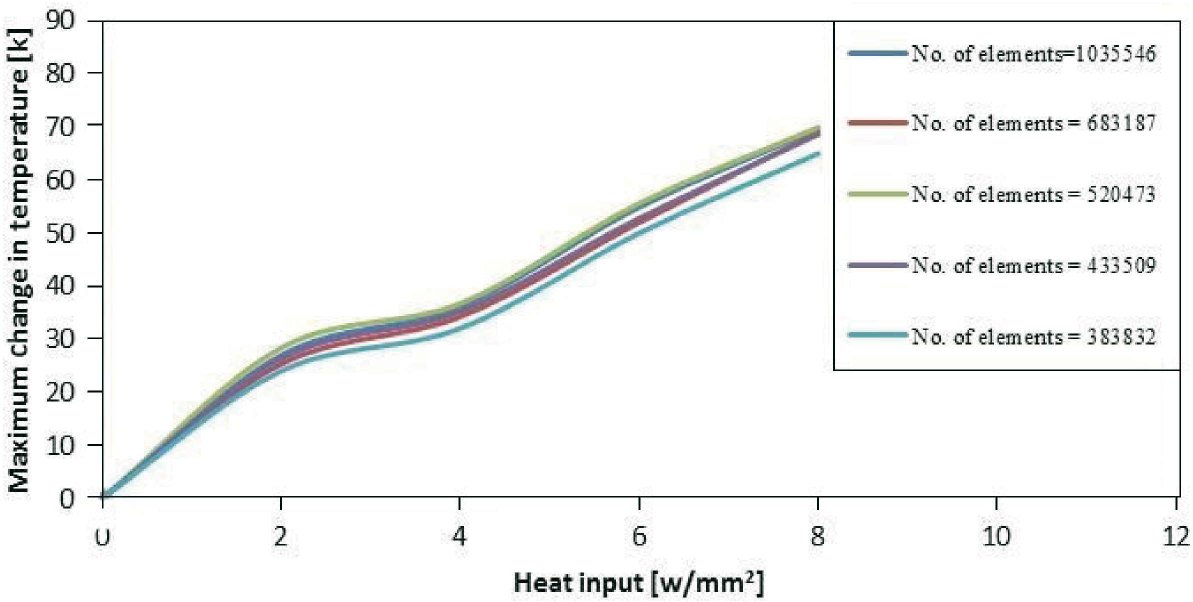

Fig. 3 Grid independence test

4.2 Model validation

The validation of the model is shown in Fig. 4 by comparing the maximum temperature change as discussed by Mihic et al. [15]. A one percent deviation of the present observations from the observations by Mihic at al. is found.

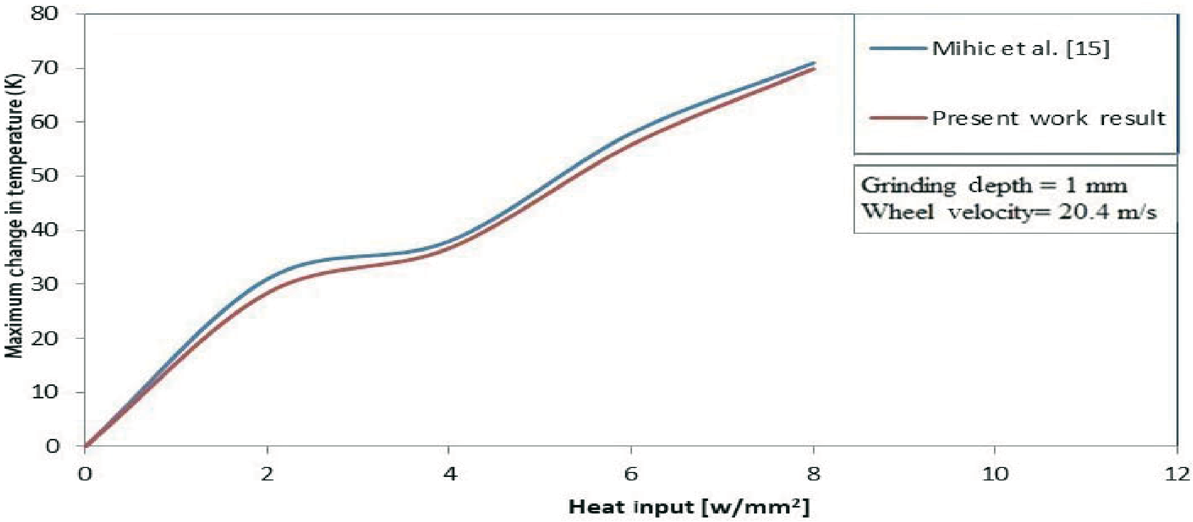

Fig. 4 Comparison of present results and results by Mihic et al. [15] for water as grinding fluid with inlet velocity 15.5 m/s

5. Result and discussion

5.1 Effect on grinding temperature at different wheel velocities and grinding depths

The numerical simulation is done for the temperature at various wheel velocities and grinding depths on an aluminium workpiece. Fig. 5 represents the variation of temperature on the workpiece surface in the grinding zone for constant wheel velocities at various depths of cut for water and kerosene oil as grinding fluids. In the case of water as a grinding fluid, as the grinding depth increases from 0.50 to 1.10 mm, the grinding temperature varies from 325 K to 370 K for a wheel velocity of 60 m/s, from 319K to 357 K for a wheel velocity of 68 m/s, and from 316 K to 347 K for a wheel velocity of 76 m/s. The temperature increases with the increasing grinding depth because the heat zone was increased. For kerosene oil, as the grinding depth varies from 0.50 to 1.10 mm, the temperature varies from 419 K to 619 K for a wheel velocity of 60 m/s, from 389K to 570 K for a wheel velocity of 68 m/s, and from 373 K to 509 K for a wheel velocity of 76 m/s. The temperature increases with the increasing grinding depth because the heat zone was increased. Hence, a further increase in temperature in the grinding zone took place; a similar trend for the workpiece temperature with depths of cut is observed at wheel velocities of 68 and 76 m/s for kerosene oil as grinding fluid.

The maximum grinding temperature for various cases can be represented by varying wheel velocities and grinding depths as shown in Fig. 6. The maximum grinding temperature decreases with increases in the wheel velocity because as the wheel velocity increases, the cutting time decreases; hence, the total strength of heat flux decreases. Fig. 7 represents the temperature distribution in the workpiece when water and kerosene oil are used as grinding fluids for wheel velocities of 60 m/s, 68 m/s, and 76 m/s, and a grinding depth of 1.10 mm. As the wheel velocity increases, the grinding temperature decreases. Mihic et al. [17] and Li et al. [22] also found that as the wheel velocity increases, the maximum grinding temperature decreases. Lavine and Jen [1] discussed the direct relation between the velocity ratio (wheel velocity to workpiece velocity) and non-dimensional temperature. Thanedar et al. [26] also observed that minimum thermal damage occurs at higher wheel speed and lower grinding depths. Gviniashvili et al. [29] suggested that increasing the wheel speed helps in increasing the useful flow rate. The high value of the useful flow rate prevents the excessive grinding temperature [30].

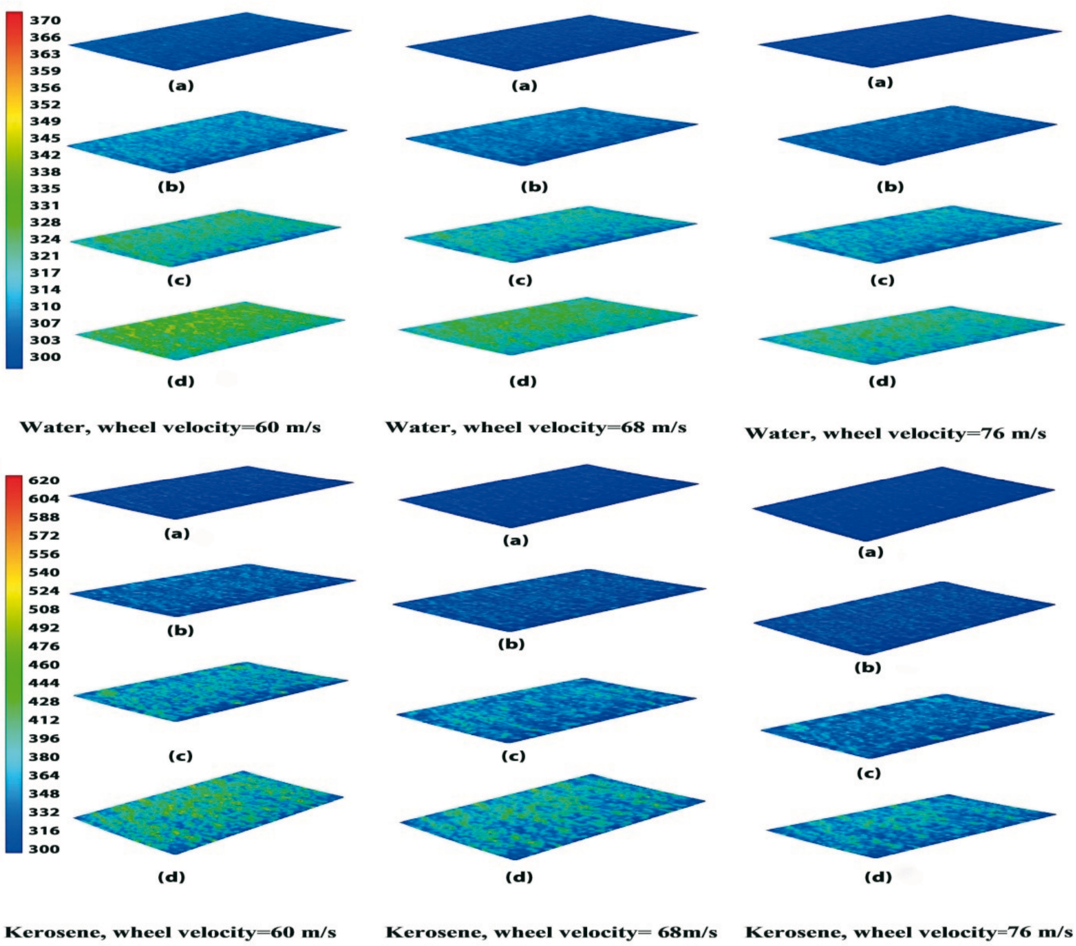

Fig. 5 Contours of total temperature (K) in grinding zone for different wheel velocities at grinding depths (a) 0.50 mm (b) 0.70 mm (c) 0.90 mm and (d) 1.10 mm

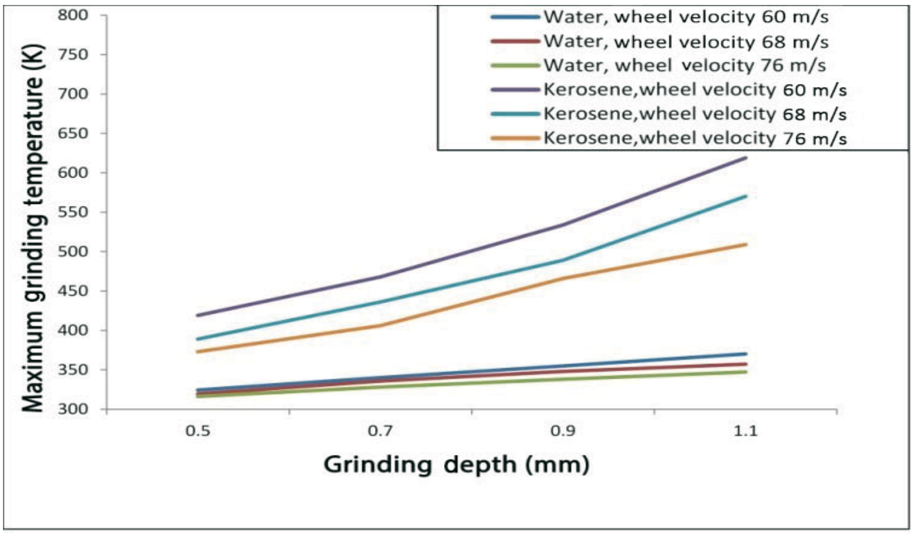

Fig. 6 Maximum grinding temperatures (K) for different grinding depths and wheel velocities using different grinding fluids

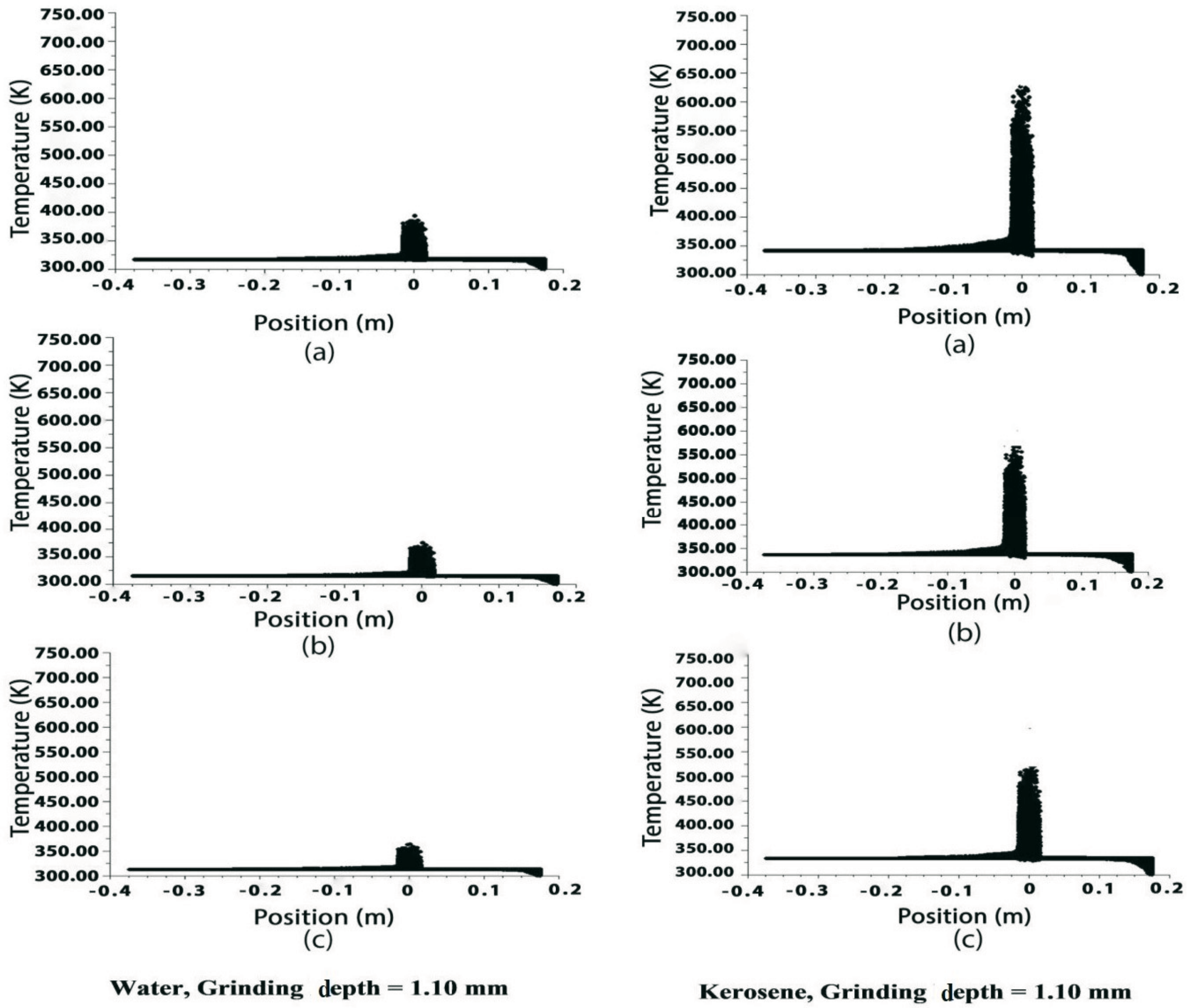

Fig. 7 Grinding temperature (K) distribution in workpiece at 1.10 mm grinding depth and wheel velocities (a) 60 m/s (b) 68 m/s (c) 76 m/s for different grinding fluids

5.2 Effect of grinding depth and wheel velocity on the coefficient of convective heat transfer of different types of grinding fluid

Fig. 8 represents the variation of the convective heat transfer coefficient of both grinding fluids for different wheel velocities and grinding depths. The convective heat transfer coefficient varies from 105,364 W/m^{2}K to 114,008 W/m^{2}K for 60 m/s wheel velocity when the grinding depth decreases from 1.10 mm to 0.50 mm for water as grinding fluid. Similarly, for 68 m/s wheel velocity, the increase in the convective heat transfer coefficient is from 116,451 W/m^{2}K to 126,004 W/m^{2}K, and for 76 m/s wheel velocity, it varies from 127,288 W/m^{2}K to 137,730 W/m^{2}K as the grinding depth decreases from 1.10 mm to 0.50 mm for the case of water as grinding fluid. The convective heat transfer coefficient increases as the grinding depth decreases from 1.10 mm to 0.50 mm. The convective heat transfer coefficient of the grinding fluid also increases as the wheel velocity increases. The convective heat transfer coefficient varies from 17,985 W/m^{2}K to 19,461 W/m^{2}K for 60 m/s wheel velocity when the grinding depth decreases from 1.10 mm to 0.50 mm for kerosene oil as grinding fluid. Similarly, for 68 m/s wheel velocity, the increase in the convective heat transfer coefficient is from 19,879 W/m^{2}K to 21,510 W/m^{2}K, and for 76 m/s wheel velocity, it varies from 21,729 W/m^{2}K to 23,512 W/m^{2}K as the grinding depth varies from 1.10 mm to 0.50 mm for kerosene oil. The convective heat transfer coefficient increases by approximately 20% when the wheel velocity increases from 60 m/s to 76 m/s. Jin and Stephenson [2] also explained that the coefficient of convective heat transfer of grinding fluids depends on wheel velocity and increases with wheel velocity.

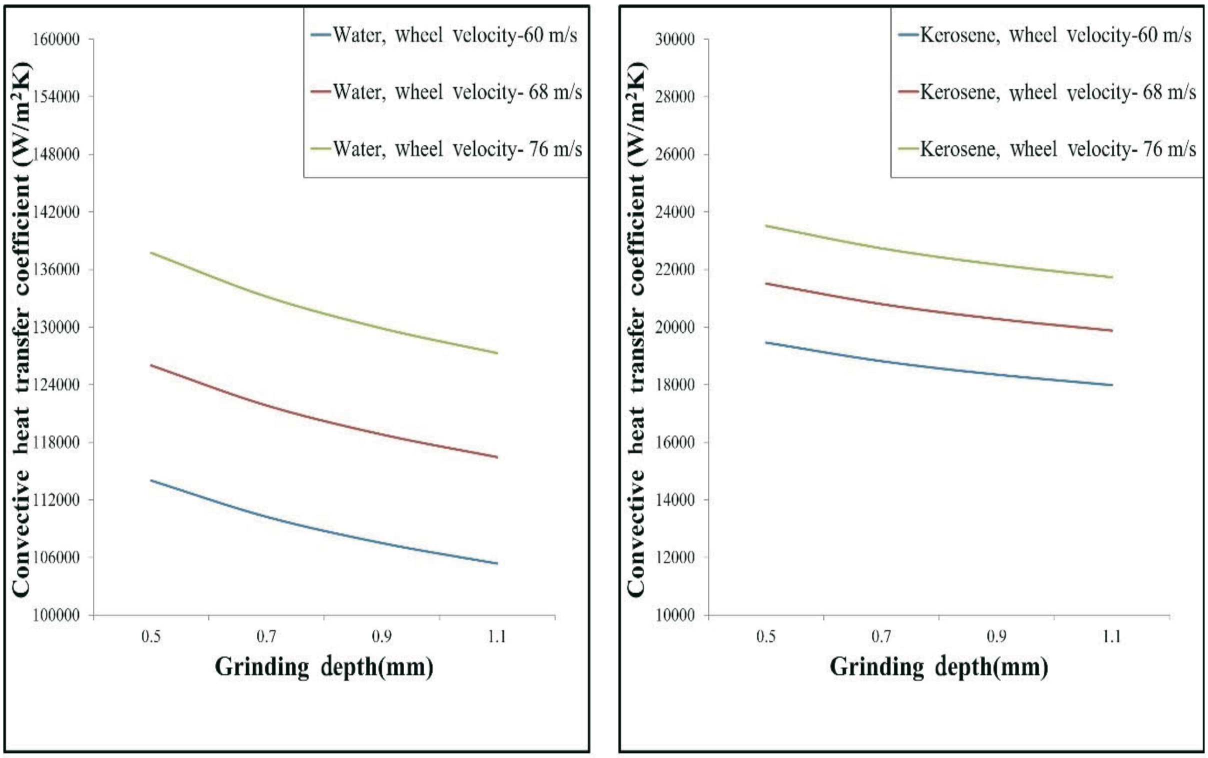

Fig. 8 Variation of convective heat transfer coefficient for different grinding depths and wheel velocities for water and kerosene oil as grinding fluids

5.3 Effect of various properties of the grinding fluid on the convection heat transfer coefficient

The effect of various properties of the grinding fluid on the convective heat transfer coefficient is studied by varying one property, and the remaining properties of kerosene are taken as given in Table 2. Fig. 9 represents the variation of the convection heat transfer coefficient of the grinding fluid for varying values of density, specific heat, viscosity, and conductivity of the grinding fluid. It is observed that there is an increase in the convection heat transfer coefficient of the grinding fluid with increases in the density of the grinding fluid. The value of the convective heat transfer coefficient increases from 16,872 W/m^{2}K to 20,167 W/m^{2}K for 60 m/s wheel velocity, from 18,646 W/m^{2}K to 22,290 W/m^{2}K for 68 m/s wheel velocity, and from 20,381 W/m^{2}K to 24,365 W/m^{2}K for 76 m/s wheel velocity when the density of the grinding fluid varies from 720 Kg/m^3 to 900 Kg/m^3. The convective heat transfer coefficient increases by 19.5 % when density is increased from 720 Kg/m^3 to 900 Kg/m^3. The convection heat transfer coefficient of the grinding fluid increases with increases in the specific heat of the grinding fluid. The value of the convection heat transfer coefficient increases from 17,840 W/m^{2}K to 18,267 W/m^{2}K for 60 m/s wheel velocity, from 19,719 W/m^{2}K to 20,191 W/m^{2}K for 68 m/s wheel velocity, and from 21,555 W/m^{2}K to 22,070 W/m^{2}K for 76 m/s wheel velocity when the specific heat of the grinding fluid varies from 2,040 J/Kg-K to 2,190 J/Kg-K. There is a very slight change in the convection heat transfer coefficient occurring with changes in the specific heat of the grinding fluid. It is observed that, as the value of viscosity increases, the value of the convection heat transfer coefficient decreases. The value of the convection heat transfer coefficient decreases from 24,854 W/m^{2}K to 16,206 W/m^{2}K for 60 m/s wheel velocity, from 27,472 W/m^{2}K to 17,913 W/m^{2}K for 68 m/s, and from

30,028 W/m^{2}K to 19,580 W/m^{2}K for 76 m/s wheel velocity when the viscosity of the grinding fluid increases from 0.0012 Kg/m-sec to 0.0030 Kg/m-sec. There is approximately a 34% decrease in the value of the convective heat transfer coefficient observed when viscosity increases in this range. The value of the convection heat transfer coefficient increases as the value of the conductivity of the grinding fluid increases. The value of the convective heat transfer coefficient increases from 13,694 W/m^{2}K to 25,327 W/m^{2}K for 60 m/s wheel velocity, from 15,137 W/m^{2}K to 27,995 W/m^{2}K for 68 m/s wheel velocity, and from 16,545 W/m^{2}K to 30,600 W/m^{2}K for 76 m/s wheel velocity when conductivity increases from 0.099 W/m-K to 0.249 W/m-K. Zhang et al. [3] also found a similar behaviour of the convective heat transfer coefficient with properties of fluids in the case of the conventional grinding process.

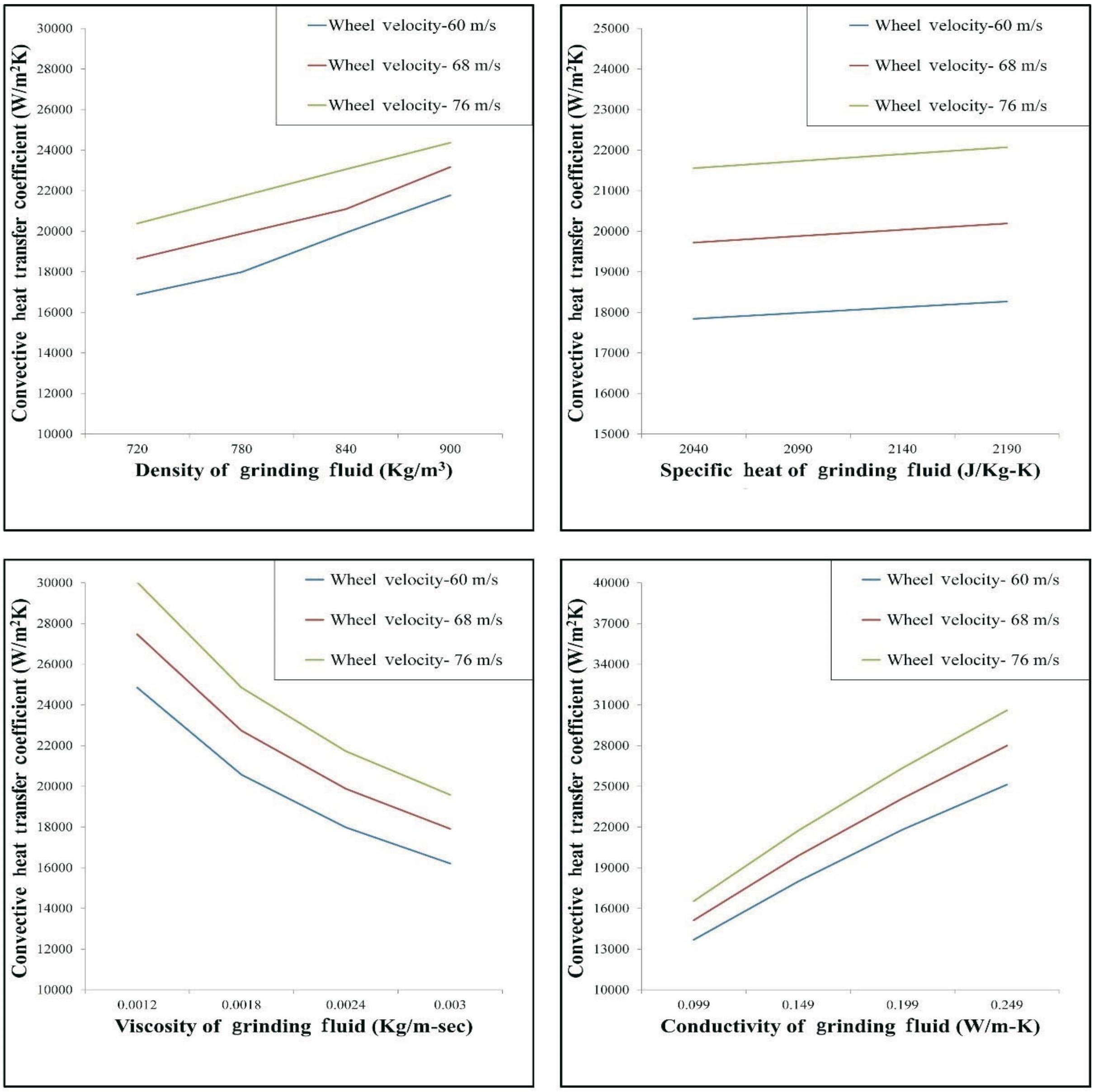

Fig. 9 Effect of grinding fluid properties on convective heat transfer coefficient of grinding fluid

It is observed that a grinding fluid that has high specific heat, density, conductivity, and lower viscosity can perform as a better coolant because of the improvement in the convective heat transfer coefficient. As shown in this study, water can be a better coolant as compared to kerosene oil because it has higher specific heat, density, conductivity, and lower viscosity than kerosene oil. Hence, in the deep grinding process, water can perform better because of better cooling properties. Ye and Pearce [28] also reported that oil-based coolants are suitable for conventional grinding processes where the grinding depth is smaller, but a water-based fluid is more suitable for deep grinding processes. This is because of lower horizontal forces in the case of oil-based coolant as compared with water. However, there are larger vertical forces in the case of oil-based coolant when compared with water, and workpiece burn can occur on the workpiece ground with an oil-based coolant. Ye and Pearce [28] also concluded that oil can give better profile retention and surface finish. However, burn in workpiece is more likely to occur with oil. A similar behaviour is observed in this study.

6. Conclusion

This paper attempts to investigate the convective heat transfer coefficient of the grinding fluid. Firstly, the maximum grinding temperature is evaluated by applying the CFD approach, and the convective heat transfer coefficient can be estimated by using the energy partition model. The main conclusions can be expressed as follows:

(1) The maximum grinding temperature depends on various manufacturing parameters of the grinding process, such as grinding depth and wheel velocity. The maximum grinding temperature varies from 325K to 370 K for the grinding depth of 0.50 to 1.10 mm at 60 m/s wheel velocity and water as grinding fluid, while in the case of kerosene oil, it varies from 419 K to 619 K for the same conditions. Hence, the maximum grinding temperature increases with an increase in grinding depth.

(2) The best way to reduce the grinding temperature in a deep grinding process is to use an appropriate grinding fluid. In the deep grinding process, the maximum grinding temperature can be reduced by increasing the convective heat transfer through the grinding fluid.

(3) It is also observed that the value of the convective heat transfer coefficient increases with an increase in wheel velocity and decreases with an increase in grinding depth.

(4) The convective heat transfer coefficient of the grinding fluid can be improved by increasing wheel velocity. It is observed that there is approximately a 20% increase in the convective heat transfer coefficient when wheel velocity increases by 60 m/s to 76 m/s.

(5) The convective heat transfer coefficient of the grinding fluid also depends on the thermo-physical properties of the grinding fluid. The value of the convective heat transfer coefficient of the grinding fluids increases with an increase in specific heat, density, and conductivity, and decreases with an increase in viscosity.

(6) These properties are important in the case of a deep grinding process to enhance the convective heat transfer through the grinding fluid. So, a grinding fluid that has high density, specific heat, conductivity, and low viscosity is preferred to be used in the deep grinding process, which means that for deep grinding processes, water-based grinding fluid is preferred.

REFERENCES

[1] Lavine A.S.; Jen T.C., Thermal aspects of grinding: heat transfer to workpiece, wheel, and fluid, *The ASME Journal of Heat and Mass Transfer* **1991**, 113(2), 296-303. https://doi.org/10.1115/1.2910561

[2] Jin T.; Stephenson D.J., A study of the convection heat transfer coefficients of grinding fluids, *CIRP Annals - Manufacturing Technology* **2008**, 57(1), 367-370. https://doi.org/10.1016/j.cirp.2008.03.074

[3] Zhang L.; Rowe W.B.; Morgan M.N., An improved fluid convection solution in conventional grinding *Proceedings of the Institution of Mechanical Engineers, Part B: Journal of Engineering Manufacture* **2013**, 227(6), 832-838. https://doi.org/10.1177/0954405413476392

[4] Jin T.; Stephenson D.J., Three dimensional finite element simulation of transient heat transfer in high efficiency deep grinding, *CIRP Annals - Manufacturing Technology* **2004**, 53(1), 259-262. https://doi.org/10.1016/S0007-8506(07)60693-3

[5] Zhang Y.; Wang C.; Zhang Y.; Meng F., Study on Temperature of Cylindrical wet grinding considering lubrication effect of grinding fluid, *International Journal of Advanced Manufacturing Technology* **2022** 121, 6095-6109. https://doi.org/10.1007/s00170-022-09658-3

[6] Peng K.; Lu P.; Lin F.; Jin T.; Bao W.; Xie G.; Shang Z., Convective cooling and heat partition to grinding chips in high speed grinding of a nickel based superalloy, *Journal of Mechanical Science and Technology* **2021** 35(6), 2755-2767. https://doi.org/10.1007/s12206-021-0545-9

[7] Rowe W.B.; Morgan M.N.; Black S.C.E.; Mills B., A simplified approach to control of thermal damage in grinding, *CIRP Annals - Manufacturing Technology* **1996** 45(1), 299-302. https://doi.org/10.1016/S0007-8506(07)63067-4

[8] Liao Y.S.; Luo S.Y.; Yanga T.H., A thermal model of the wet grinding process, Journal of Materials Processing Technology **2000**, 101, 137-145. https://doi.org/10.1016/S0924-0136 (00)00440-4

[9] Marios D.D.; Lavine A.S., Thermal aspects of grinding: the case of upgrinding, *ASME Journal of Manufacturing Science & Engineering* **2000**, 122(4), 605-611. https://doi.org/10.1115/1.1285877

[10] O'Donovan T.S.; Murray D.B.; Torrance A.A., Jet heat transfer in the vicinity of a rotating grinding wheel, *Proceedings of the Institution of Mechanical Engineers, Part C: Journal of Mechanical Engineering Science* **2006**, 220, 837-845. https://doi.org/10.1243/09544062JMES215

[11] Tu L.; Li J.; Shi W., Investigation on experiment and simulation of the grinding process of cast iron, Proc *Proceedings of the Institution of Mechanical Engineers, Part C: Journal of Mechanical Engineering Science* **2020**, 234(13), 2653-2661. https://doi.org/10.1177/0954406220907928

[12] Upadhyaya R.P.; Malkin S., Thermal aspects of grinding with electroplated CBN wheels, *ASME Journal of Manufacturing Science & Engineering* **2004**, 126(1), 107-114. https://doi.org/10.1115/1.1644547

[13] Schieber C.; Hettig M.; Zaeh M.F.; Heinzel C., 3D modeling and simulation of thermal effects during profile grinding, *Production Engineering* **2020**, 14:655-66. https://doi.org/10.1007/s11740-020-00983-8

[14] Lin B.; Morgan M.N.; Chen X.W.; Yang Y.K., Study on the convection heat transfer coefficient of coolant and the maximum temperature in the grinding process, *The International Journal of Advanced Manufacturing Technology* **2009**, 42, 1175-1186. https://doi.org/10.1007/s00170-008-1668-1

[15] Mihic S.; Cioc S.; Marinescu I.; Weismiller M.C., Detailed Study of Fluid Flow and Heat Transfer in the Abrasive Grinding Contact Using Computational Fluid Dynamics Method, *ASME Journal of Manufacturing Science & Engineering* **2013**, 135, 041002-1. https://doi.org/10.1115/1.4023719

[16] Gupta P.K.; Yadav N.P., Computational analysis for thermal behaviour of different types of Steels in grinding process, *Proceedings of ICMET, Smart Innovation, Systems and Technologies* **2020**, 174, 169-180. https://doi.org/10.1007/978-981-15-2647-3_16

[17] Mihic S.; Cioc S.; Marinescu I.; Weismiller M.C., 3D CFD Parametric Study of the Impact of the Fluid Properties and Delivery Conditions on Flow and Heat Transfer in Grinding, *Advanced Materials Research* **2011**, 325: 225-230. https://doi.org/10.4028/www.scientific.net/AMR.325.225

[18] Jamshidi H.; Budak E., A 3D analytical thermal model in grinding considering a periodic heat source under dry and wet conditions, *Journal of Materials Processing Technology* **2021**, 295, 117158. https://doi.org/10.1016/j.jmatprotec.2021.117158

[19] Gupta P.K.;, Yadav N.P., Computational investigation for structural behavior in deep grinding process, *Journal of the Brazilian Society of Mechanical Sciences and Engineering* **2023**, 45, 279. https://doi.org/10.1007/s40430-023-04201-1

[20] Xiao G.; Zhao B.; Ding W.; Huan H., On the grinding performance of metal-bonded aggregated cBN grinding wheels based on open-pore structures, *Ceramics International* **2021**, 47(14), 19709-19715. https://doi.org/10.1016/j.ceramint.2021.04.001

[21] Row W.B.; Morganl M.N.; Batakol A.; Jin T., Energy and temperature analysis in grinding, *Transactions on Engineering Sciences* **2003**, 44, 3–24

[22] Li B.K.; Miano Q.; Li M.; Zhang X.; Ding W.F., An investigation on machined surface quality and tool wear during creep feed grinding of powder metallurgy nickel-based super alloy FGH96 with alumina abrasive wheels, *Advances in Manufacturing* **2020**, 8, 160-176. https://doi.org/10.1007/s40436-020-00305-2

[23] Ansys,Inc.,,FLUENT 19.0 R3 User‘s Guide, Canonsburg, PA

[24] Jamshidi H.; Budak E., On the prediction of Surface burn and its thickness in grinding processes. CIRP Annals Manufacturing Technology **2021**, 70(1), 285-288. https://doi.org/10.1016/j.cirp.2021.04.041

[25] Ma X.; Yao B.; Cai Z.; Li Z.; Li Z.; Chen G.; Liu W., Temperature field responses to face gear grinding conditions based on a comprehensive force–thermal model, *Precision Engineering* **2023**, 83, 22-41. https://doi.org/10.1016/j.precisioneng.2023.05.004

[26] Thanedar A.; Dongre G.G.; Joshi S.S., Analytical Modelling of Temperature in Cylindrical Grinding to Predict Grinding Burns, *International Journal of Precision Engineering and Manufacturing* **2019**, 20, 13-25. https://doi.org/10.1007/s12541-019-00037-9

[27] Zhang L.; Rowe W.B., Study of Convective Heat Transfer in Grinding Applied to Tool Carbide, *ASME Journal of Manufacturing Science & Engineering* **2020**, 142(2), 021001. https://doi.org/10.1115/1.4045598

[28] Ye NE and Pearce TRA, A Comparison of Oil and Water as Grinding Fluids in the Creep Feed Grinding Process, *Proceedings of the Institution of Mechanical Engineers, Part B: Journal of Engineering Manufacture* **1984**, 198 (4), 229-237. https://doi.org/10.1243/PIME_PROC_1984_198_073_02

[29] Gviniashvili V.K.; Woolley N.H.; Rowe W.B., Useful coolant flowrate in grinding, *International Journal of Machine Tools & Manufacture*, **2004**, 44, 629–636. https://doi.org/10.1016/j.ijmachtools.2003.12.005

[30] Li C.; Zhang X.; Zhang Q.;Wang S.; Zhang D.; Jia D.; Zhang Y., Modeling and simulation of useful fluid flow rate in grinding, *The International Journal of Advanced Manufacturing Technology*, **2014**, 75, 1587-1604. https://doi.org/10.1007/s00170-014-6257-x

[31] Barjasic D.; Stegic M.; Juran M., Numerical Evaluation of Plane Grinding Stability, *Transactions of Famena* **2023**, vol 47(1) , 13-20. https://doi.org/10.21278/TOF.471046522

[32] Todic A.; Djordjevic MT.; Arsic D.; Dzunic D.; Lazic V.; Aleksandrovic S.; Krstic B., Influence of Vanadium content of the tribological behaviour of X140CrMo12-1 Air hardening steel, *Transactions of Famena,* **2022**, vol 46(2), 15-22. https://doi.org/10.21278/TOF.462035021

[33] Li Z.; Gao Z.; An Z.; Sun Y.; Wu B.; Zhai Y., A novel temperature model of regions formed during the preheating stage of belt heating in incremental Sheet forming, *Transactions of Famena,* **2023**, vol 47(4), 1-12. https://doi.org/10.21278/TOF.474053423

[34] Chen J.Y.; Lin Y.L.; Lee B.Y., Prediction model of end mill cutting edge based on material properties and cutting conditions, *Transactions of Famena*, **2022**, vol 46(2), 69-84. https://doi.org/10.21278/TOF.462033821

Submitted: 03.07.2023
Accepted: 15.11.2023

Puneet Kumar Gupta*, Research Scholar
N.P. Yadav, Professor
Department of Mechanical Engineering,
BIET, Jhansi, India
*Corresponding author:
puneetguptably89@gmail.com